

# Binary Mixtures of SH- and CH<sub>3</sub>-Terminated Self-Assembled Monolayers to Control the Average Spacing Between Aligned Gold Nanoparticles

Asad Rezaee · Laura C. Pavelka · Silvia Mittler

Received: 21 May 2009 / Accepted: 17 July 2009 / Published online: 2 August 2009  
© to the authors 2009

**Abstract** This paper presents a method to control the average spacing between organometallic chemical vapor deposition (OMCVD) grown gold nanoparticles (Au NPs) in a line. Focused ion beam patterned CH<sub>3</sub>-terminated self-assembled monolayers are refilled systematically with different mixtures of SH- and CH<sub>3</sub>-terminated silanes. The average spacing between OMCVD Au NPs is demonstrated systematically to decrease by increasing the v/v% ratio of the thiols in the binary silane mixtures with SH- and CH<sub>3</sub>-terminated groups.

**Keywords** Average spacing · FIB · Gold · Nanoparticle · OMCVD · Self-assembly

## Introduction

Along with the other applications, recent years have seen a tremendous impact on gold nanoparticle (Au NP) optical response in biological assays, detection, labeling, and sensing [1]. It is of great importance to observe a pronounced shift in the localized surface plasmon resonance (LSPR) corresponding to an absorption peak intrinsic to Au NPs, upon binding of a material onto Au NPs [2].

However, to achieve such a pronounced LSPR shift—when only a minute amount of sample material is available, or in a screening approach with many different recognition agents—the volume has to be minimized and the accessibility of the analyte to the Au NPs has to be enhanced. Therefore, two-dimensional approaches with organometallic chemical vapor deposited (OMCVD) Au NPs on a surface are envisaged [3].

The spectral location ( $\lambda_{\text{max}}$ ) and width of the LSPR peak can be optimized for sensor applications by controlling average spacing [4]. In contrast, the LSPR peak of randomly positioned Au NPs can be fairly broad [5]. As a result, a sensor fabricated with Au NPs with a narrow and spectrally well-located LSPR peak shows a clearer peak shift ( $\Delta\lambda_{\text{max}}$ ) improving the sensitivity. We have recently introduced a new method to align OMCVD-grown Au NPs via focused ion beam (FIB) nano-lithography on a self-assembled monolayer (SAM) functionalized substrates and refilling the structures with a pure SH-terminated silane SAM [6]. It was concluded that the average spacing between Au NPs can be controlled by varying the FIB dose. In the present work, we follow an alternative route with the dilution of the re-filling SAM to control the availability of nucleation sites to bind Au NPs.

Mercapto or thiol groups (–SH) have been used as nucleation sites for the OMCVD of Au NPs [7, 8]. 3-Mercaptopropyltrimethoxysilane (MPTS), which provides monolayers presenting –SH reactive group, was diluted with octadecyltrichlorosilane (OTS) as a non-reactive site for the OMCVD process with the Au precursor (trimethylphosphinegoldmethyl) [9]. It has been demonstrated that OTS with a CH<sub>3</sub>-terminal function is a reliable resist for Au OMCVD [10, 11]. Here, OTS plays two roles: a resist SAM to be patterned by FIB and a dilution in the binary mixture solutions of MPTS and OTS to refill the

---

A. Rezaee · S. Mittler (✉)  
Department of Physics and Astronomy, The University  
of Western Ontario, London, ON N6A 3K7, Canada  
e-mail: smittler@uwo.ca

A. Rezaee  
e-mail: arezaee@uwo.ca

L. C. Pavelka  
Department of Chemistry, The University of Western Ontario,  
London, ON N6A 5B7, Canada  
e-mail: lcpavelk@uwo.ca

patterned lines to control the density of functional SH-groups for Au NP nucleation.

## Experimental Section

### Materials

P-type silicon <100> wafers were purchased from Silicon Valley Microelectronics Inc. (CA, USA) and used as substrates. OTS ( $\text{Cl}_3\text{-Si-(CH}_2\text{)}_{17}\text{-CH}_3$ , 90+%) and MPTS ( $\text{HS-(CH}_2\text{)}_3\text{-Si-(O-CH}_3\text{)}_3$ ,  $\geq 97.0\%$ ) were purchased from Sigma-Aldrich and used without further purification. Anhydrous ethanol (99+%, Commercial Alcohols Inc.) was used without further purification.

### OTS SAM Preparation as a Resist

Silicon wafers were cleaved into pieces of  $1\text{ cm} \times 1\text{ cm}$ . Before the silanization process, substrates were first cleaned by ultrasonication in a 2% solution of Hellmanex (Hellma, Germany), acetone, and MilliQ water (Milli-Q,  $\rho \geq 18\text{ M}\Omega\text{cm}$ , Millipore) each for 5 min and rinsed five times with MilliQ water between each step. They were immersed in a 4:1 mixture of concentrated  $\text{H}_2\text{SO}_4$  and  $\text{H}_2\text{O}_2$  overnight, washed with copious amounts of MilliQ water, and dried with  $\text{N}_2$ . Contact angle measurements (Goniometer Model 200, Ramé-Hart Instrument Co., Netcong, NJ) confirmed the hydrophilic nature of the silicon substrates ( $\theta < 2^\circ$ ).

A 10 mM solution of OTS in anhydrous toluene was prepared. Since OTS is easily hydrolyzed with the atmospheric moisture, this solution was always prepared under nitrogen atmosphere (glove box) and used immediately. After 6 h assembly time, the samples were taken out of the OTS solution, rinsed with toluene and ethanol, and placed in a vacuum oven at  $120^\circ\text{C}$  for 1 h (20 min heating + 40 min under vacuum). At this point, contact angle measurement confirmed hydrophobic layers formed on the silicon substrates ( $\theta_{\text{avg}} \approx 110^\circ$ ). The freshly prepared silane SAMs were used immediately as substrates for FIB nanolithography.

### Mixed MPTS and OTS SAM Refilling

The patterned samples were rinsed and ultrasonicated in ethanol for 1 min. Stock solutions of 1% MPTS and 10 mM OTS in ethanol were prepared. Mixtures with 20, 40, 60, 80, 100% volume ratios of MPTS in OTS solution were made inside the glove box. Three hours of immersion was carried out at room temperature to refill the “empty surface” and supply nucleation sites for the Au OMCVD process. After removing the sample from the mixture

solutions, they were rinsed and ultrasonicated with ethanol, dried with  $\text{N}_2$ , and subsequently baked in a vacuum oven at  $94^\circ\text{C}$  for 1 h (20 min heating + 40 min under vacuum).

The temperature that most silane SAMs can form a covalent attachment to the surface is  $120^\circ\text{C}$ . Our previous experiments on MPTS indicated that the baking temperature for MPTS is related to the viability of the thiol groups ( $-\text{SH}$ ). We found that  $94^\circ\text{C}$  is the optimum temperature, at which MPTS can still have a covalent bonding onto the oxide surface and the  $-\text{SH}$  head groups are still intact, whereby Au NPs bond onto the thiols.  $120^\circ\text{C}$  was also tried for MPTS, but most of the time, Au NPs did not bind to the SAMs anymore. Apparently, most of thiols were oxidized at  $120^\circ\text{C}$ .

### Au OMCVD

The vapor deposition of gold via the  $[(\text{CH}_3)_3\text{P}]\text{AuCH}_3$  precursor onto the MPTS/OTS SAMs was carried out in a vacuum-sealed glass reactor chamber, which contained the samples and a small glass vessel with 20 mg of the Au precursor. The reactor was evacuated ( $p_{\text{min}} \cong 0.05\text{ hPa}$ ) for 30 min and then placed in an oven at  $\sim 65^\circ\text{C}$  for 30 min.

### FIB and SEM

Sub-100 nm lateral resolution 30 kV  $\text{Ga}^+$  bombardment experiments were carried out by a Leo/Zeiss 1540 FIB/SEM (LEO Electron Microscope, Zeiss, Germany) at a beam current of 5 pA. Pattern design and FIB control were performed by *DesignCAD* and *NPGS* software, respectively [12, 13]. SEM images were obtained at 3.00 kV electron accelerating voltage operating condition. No conductive coating was applied on any sample. Image processing on the SEM images was performed by *ImageJ* software [14].

## Results and Discussion

In order to align the OMCVD Au NPs, OTS-covered silicon surfaces were FIB nanolithography patterned [6]. As shown in Fig. 1, the pattern consists of 16 sets of lines representing different doses. The lines were refilled with different volume% ratios of SH-/ $\text{CH}_3$ -terminated silanes in binary mixture solutions of MPTS and OTS. The OMCVD process was performed to grow Au NPs into the lines. An SEM image depicting the aligned Au NPs is shown in Fig. 1.

The MPTS molecules can ideally only bind to FIB-irradiated lines, where the  $\text{CH}_3$ -terminated molecules of self-assembled OTS are totally eradicated or where the

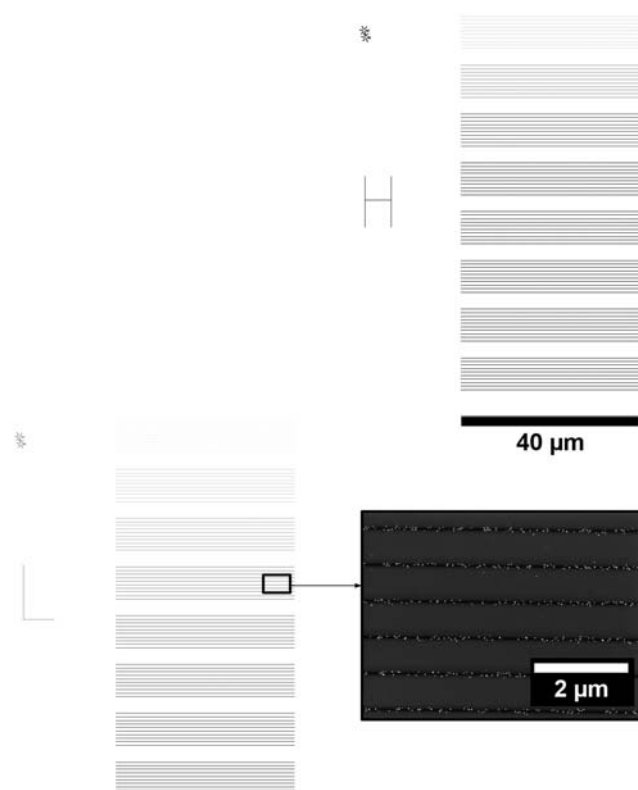


**Fig. 1** Pattern for FIB nanolithography on each sample including 16 different doses: “L” (lower doses) 0.5, 1, 2, 3, 4, 5, 5.5, 6 nC/cm and “H” (higher doses) 6.5, 7, 7.5, 8, 8.5, 9, 10, 11 nC/cm (top to bottom); along with the SEM image of OMCVD-grown Au NPs on refilled lines with 80 v/v% of MPTS and FIB irradiated at 3 nC/cm

octyl groups of OTS are removed. In the latter case, the exposed Si remaining from the FIB-irradiated OTS molecule can bind to MPTS. The damaged alkyl groups or partly destroyed OTS molecules are most likely oxidized to COH, COOH, etc., where Au NPs can grow onto. Therefore, a sample without refilling was prepared and compared with the samples refilled with diluted MPTS. In the presence of immobilized MPTS, OMCVD Au grows mainly onto the SH-groups [7, 8]. It was expected that by diluting the solution providing thiols, the nucleation sites available for Au OMCVD are reduced, and therefore, the number of Au NPs grown onto the refilled lines decreases. This will result in an increase in the average spacing between Au NPs.

Figures 2 and 3 show the Au NPs formed onto the refilled SAMs in the lines irradiated at the first two lowest doses (0.5 and 1.0 nC/cm). Each line in the SEM images corresponds to a volume% of refilled MPTS. It can clearly be seen in Figs 2 and 3 that the density of Au NPs increased by refilling the lines with increasing v/v% ratios of MPTS, as expected. However, without refilling the Au NP density was the highest. The lateral sizes of Au NPs were constant at diameters of  $\sim 24$  nm. At lower doses

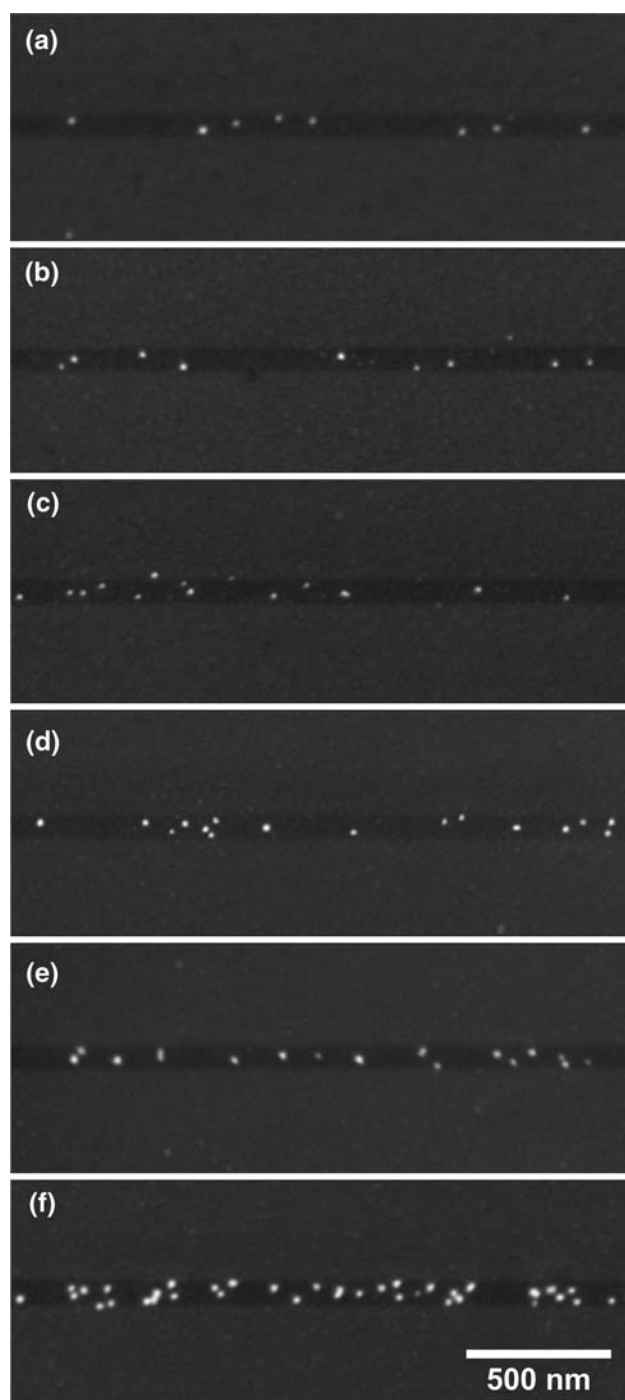


**Fig. 2** SEM images of FIB nanolithography aligned Au NPs at a dose of 0.5 nC/cm refilled with (a) 20 v/v%, (b) 40 v/v%, (c) 60 v/v%, (d) 80 v/v%, (e) 100 v/v% of MPTS, and (f) without any refilling

(less than  $\sim 7$  nC/cm), the density of Au NPs is relatively more sensitive to the refilled binary mixture. It was found that there is a dose threshold ( $\sim 7$  nC/cm), at which all the OTS SAMs are removed [6]. By applying higher doses, the availability to bind the refilling SAMs will not change because the incoming refilling molecules bond to

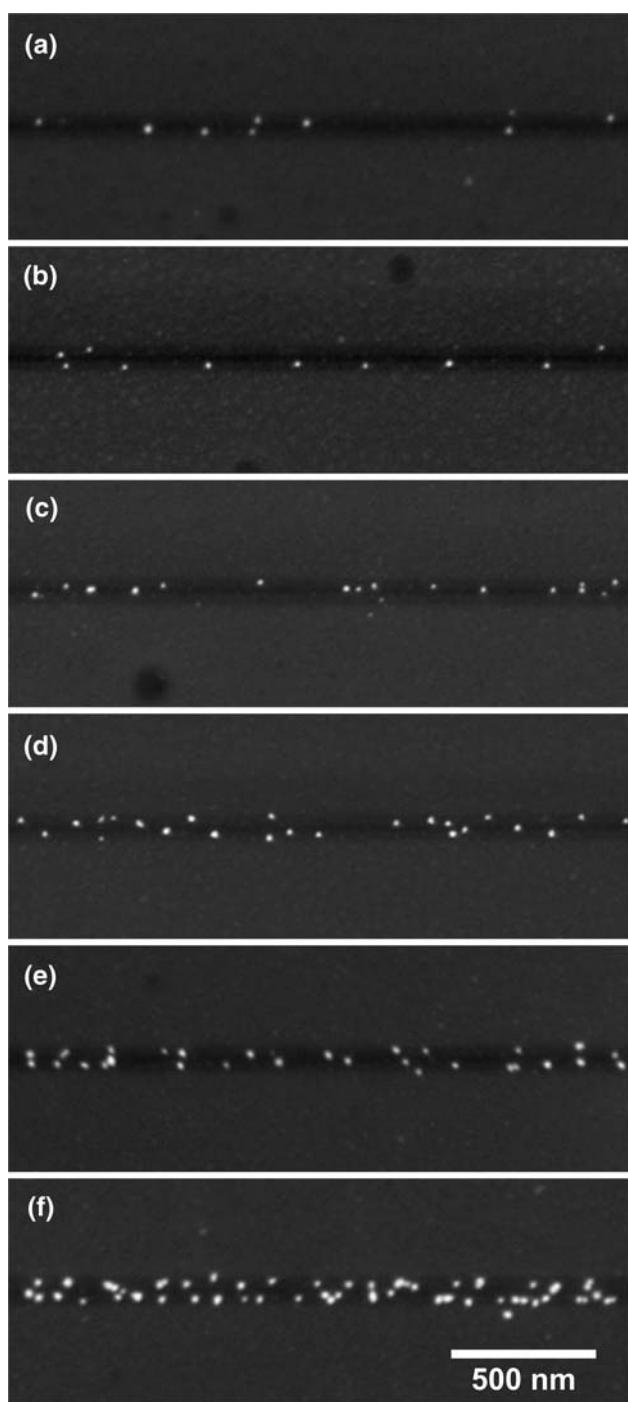


**Fig. 3** SEM images of FIB nanolithography aligned Au NPs at a dose of 1 nC/cm refilled with (a) 20 v/v%, (b) 40 v/v%, (c) 60 v/v%, (d) 80 v/v%, (e) 100 v/v% of MPTS, and (f) without any refilling

completely “empty” silica surfaces. Therefore, partially removed OTS SAMs remained in the lines after FIB irradiation can improve the control of density and average spacing between Au NPs by varying the v/v% ratios.

In order to calculate the average center-to-center spacing, the Au NP coordinates along three selected 6- $\mu$ m lines

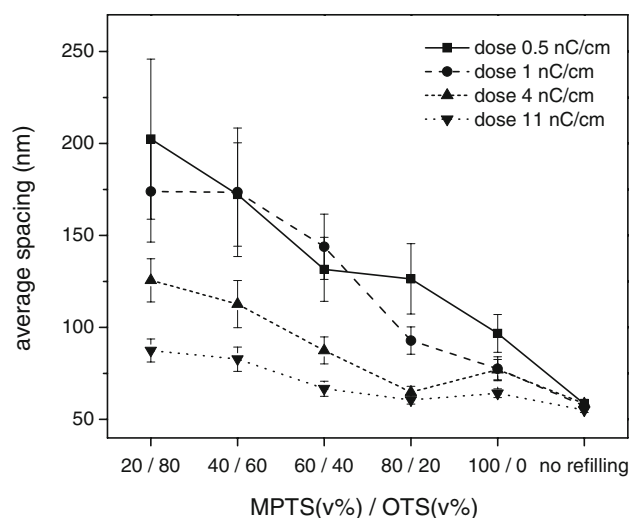


**Fig. 4** Average center-to-center spacing between aligned Au NPs at doses of 0.5, 1.0, 4.0, and 11 nC/cm versus the v/v% ratio of MPTS/OTS binary mixture. The error bars represent the standard errors of the mean of the NNDs

in each SEM image were recorded. The nearest neighbor distances (NNDs) between Au NPs in each line were calculated and averaged. Averages of NNDs (average spacing) versus v/v% ratio are depicted in Fig. 4. Although all the 16 doses yielded a general decrease in NND with increasing MPTS v/v% ratio, four doses (0.5, 1.0, 4.0, and 11 nC/cm) were selected for Fig. 4. Again, almost the same decreasing trend (the same slope, if linear fitting applied) was observed for doses higher than the threshold. The difference between minimum and maximum average spacing of Au NPs grown onto 20 and 100 v/v% of refilling MPTS was 106, 96, 49, and 23 nm for doses 0.5, 1.0, 4.0, and 11 nC/cm, respectively. This confirms that lower doses are more sensitive to v/v% ratio changes, as the slopes confirm in Fig. 4.

The “last point” on the x-axis in Fig. 4 refers to “no refilling”, which indicates the average spacing between Au NPs grown on FIB-irradiated lines without any refilling SAM. In comparison with –SH refilling, the average spacing for the sample without refilling did not change with respect to the FIB dose. The “no refilling” can be considered as a “saturated” state, in which the density of OMCVD-grown Au NPs is maximized and constant. As an example, the difference between minimum and maximum averages spacing with respect to the FIB dose for the sample refilled with 20 v/v% of MPTS was 121 nm, while it was only 4 nm for the sample without refilling. It is, therefore, concluded that the reason for the average spacing control of the aligned OMCVD Au NPs with MPTS refilling at a fixed dose is due to the density control of the thiols in the binary mixture solution of SH- and CH<sub>3</sub>-terminated silanes.

## Conclusions

We have introduced a method to control the average spacing between aligned OMCVD-grown Au NPs by varying the volume% of SH-terminated silane in a binary mixture of SH- and CH<sub>3</sub>-terminated groups. CH<sub>3</sub>-terminated molecules were used to dilute and control the density of available thiols in refilling SAMs for OMCVD Au growth. The FIB dose dependence of average spacing was previously demonstrated. Here, SEM image analyses indicated that the average spacing between aligned Au NPs at a fixed dose can effectively be controlled by changing the v/v% ratio of SH-groups. The average spacing decreased with higher v/v% ratios.

**Acknowledgments** The authors would like to thank Ontario Centers of Excellence (OCE, MMO/SC60134, and BM60148), Canada Foundation for Innovation (CFI), Ontario Innovation Trust (OIT), Ontario Photonics Consortium (OPC), and CRC Program of the Government of Canada for their kind financial support and the Western Nanofabrication Facility for the availability of FIB and SEM. We also thank Todd Simpson and David R. Tessier for their help. Kim Baines from the Department of Chemistry is thanked for the availability of the facilities to synthesize the precursor.

## References

1. A.J. Haes, D.A. Stuart, S.M. Nie, R.P. Van Duyne, J. Fluoresc. **14**, 355 (2004). doi:[10.1023/B:JOFL.0000031817.35049.1f](https://doi.org/10.1023/B:JOFL.0000031817.35049.1f)
2. P. Rooney, A. Rezaee, S. Xu, T. Manifar, A. Hassanzadeh, G. Podoprygorina, V. Böhmer, C. Rangan, S. Mittler, Phys. Rev. B. **77**, 235446 (2008). doi:[10.1103/PhysRevB.77.235446](https://doi.org/10.1103/PhysRevB.77.235446)
3. A.K.A. Aliganga, I. Lieberwirth, G. Glasser, A.S. Duwez, Y.Z. Sun, S. Mittler, Org. Electron. **8**, 161 (2007). doi:[10.1016/j.orgel.2006.09.002](https://doi.org/10.1016/j.orgel.2006.09.002)
4. K.H. Su, Q.H. Wei, X. Zhang, J.J. Mock, D.R. Smith, S. Schultz, Nano Lett. **3**, 1087 (2003). doi:[10.1021/nl034197f](https://doi.org/10.1021/nl034197f)
5. S. Link, M.A. El-Sayed, J. Phys. Chem. B. **103**, 8410 (1999). doi:[10.1021/jp9917648](https://doi.org/10.1021/jp9917648)
6. A. Rezaee, A.K.A. Aliganga, L.C. Pavelka, S. Mittler, Adv. Mater.: Chem. Vapor Deposit. (in preparation) (2009)
7. J. Käshammer, P. Wohlfart, J. Weiss, C. Winter, R. Fischer, S. Mittler-Neher, Opt. Mater. **9**, 406 (1998). doi:[10.1016/S0925-3467\(97\)00105-5](https://doi.org/10.1016/S0925-3467(97)00105-5)
8. P. Wohlfart, J. Weiss, J. Käshammer, C. Winter, V. Scheumann, R.A. Fischer, S. Mittler-Neher, Thin Solid Films. **340**, 274 (1999). doi:[10.1016/S0040-6090\(98\)01366-2](https://doi.org/10.1016/S0040-6090(98)01366-2)
9. A.K.A. Aliganga, A.S. Duwez, S. Mittler, Org. Electron. **7**, 337 (2006). doi:[10.1016/j.orgel.2006.03.013](https://doi.org/10.1016/j.orgel.2006.03.013)
10. T. Manifar, A. Rezaee, M. Sheikhzadeh, S. Mittler, Appl. Surf. Sci. **254**, 4611 (2008). doi:[10.1016/j.apsusc.2008.01.100](https://doi.org/10.1016/j.apsusc.2008.01.100)
11. A. Rezaee, K.K.H. Wong, T. Manifar, S. Mittler, Surf. Interface Anal. (2009). doi: [10.1002/sia.3073](https://doi.org/10.1002/sia.3073)
12. *Design CADLT 2000*. (Upperspace Corporation, Pryor, OK, 2000)
13. J. Nabity, *Nanometer Pattern Generation System (NPGS) 9.0.107* (JC Nabity Lithography Systems, Bozeman, MT, 2002)
14. W.S. Rasband, *ImageJ 1.41e* (National Institutes of Health, Bethesda, Maryland, USA, 2008), <http://rsb.info.nih.gov/ij/>